Quantitative explanation of the Schottky barrier height

Raymond T. Tung [1,*] and Leeor Kronik [2,†]

[1]*Department of Physics, Brooklyn College, CUNY, Brooklyn, New York 11210, USA*
and Physics Ph.D. Program, Graduate Center, CUNY, New York, New York 10016, USA
[2]*Department of Materials and Interfaces, Weizmann Institute of Science, Rehovoth 76100, Israel*

Eight decades ago, Schottky proposed that the energy barrier at the metal-semiconductor interface, which now bears his name, should be compared with the difference of two surface quantities, the work function (WF) of the metal and the ionization potential of the semiconductor. This tradition of plotting and modeling the Schottky barrier height (SBH) against the metal WF has been followed ever since. However, success in general quantitative understanding of the SBH from physical principles has been limited, and empirical models are still relied upon. Here, we show that the stumbling block that has prevented a broadly applicable physical explanation of the SBH is the presence of surface dipole terms, inherently included in the traditional, Schottky-Mott styled analyses. By removing these surface contributions with the help of the recently developed neutral polyhedra theory, we show that the SBHs calculated for a very large number of epitaxial interfaces between metals and zinc-blende semiconductors are quantitatively explained from general chemical principles. Amazingly, SBHs calculated for 17 different semiconductors fit onto the same universal plot. Previously, SBHs needed to be grouped according to the semiconductor before analyses could be conducted separately for, and with empirical parameters specific to, each semiconductor. This work shows that the mechanism for SBH formation at metal-semiconductor interface is none other than the same chemistry responsible for charge distribution in molecules. There is no need for empirical modeling once the traditional beginning-point of SBH analysis is abandoned and the proposed new one is used.

The Schottky barrier, which controls carrier transport at the interface between a metal and a semiconductor, is ubiquitous in electronic devices. The formation mechanism of the SBH has been the focus of both basic and applied research for decades [1–3]. Early experiments conducted on polycrystalline metal-semiconductor (MS) interfaces revealed an insensitivity of the SBH to the metal work function (WF), a phenomenon known as Fermi-level pinning [4–6]. This led to a host of empirical models, centered around a charge-neutrality level (CNL) of the semiconductor, which supposedly pins the Fermi level [4,7–9]. However, a strong dependence of the SBH on the orientation and structure of epitaxial MS interfaces was discovered [10–13], illustrating that the Fermi level is actually unpinned and that the SBH at polycrystalline interfaces is spatially inhomogeneous [11,14–17]. For selected epitaxial MS interfaces, first-principles calculations, based on density-functional theory (DFT), have confirmed the dependence of SBH on the interface atomic structure [18–23]. Even though the magnitude of the SBH is a direct consequence of charge distribution at the MS interface, and the latter is governed by chemistry, it has not been possible to predict the SBH quantitatively from chemical principles [3]. Here, through calculations conducted on epitaxial interfaces between metals and zinc-blende/diamond (ZBD) semiconductors, the stumbling block that has thus far prevented a general quantitative explanation of the SBH from scientific principles is identified and removed. From this beginning point, quantitative explanation of a large number of SBH is realized, with the same chemical principle that explains charge distribution in molecules.

The beginning point for nearly all SBH analyses has been the Schottky-Mott theory (SMT) [24,25], which assumes that the relative position of the semiconductor and metal bands at the interface is the same as that for their respective free surfaces. The SBH for a *p*-type semiconductor, $\phi_{B,p}$, is then simply given by the difference between the ionization potential (IP) of the semiconductor, I_{SC}, and the WF of the metal, ϕ_M, i.e., $\phi_{B,p}(SMT) = I_{SC} - \phi_M$ Clearly, charge redistribution at the interface-specific region (ISR) between the semiconductor and metal takes place and leads to a correction to SMT, in the form of an electrostatic dipole, Δ_{ISR}. Therefore,

$$\Phi_{B,P} = I_{SC} - \Phi_M + \Delta_{ISR} \qquad (1)$$

is the equation that has been used almost exclusively to model the SBH, and it is also the origin of the problem! Because both I_{sc} and ϕ_M contain surface-dipole contributions unconnected with properties of the MS interface, Δ_{ISR} must somehow cancel these surface contributions in order for Eq. (1) to be accurate. Naturally, Δ_{ISR} cannot be easily modeled from chemical principles alone. This forced researchers to largely abandon the chemical route of modeling the interface dipole and resort to empirical models of SBH [8,9].

A systematic way out of this quandary is made possible by using the proposed neutral polyhedra theory (NPT) [26–28] to remove the surface-dipole contributions to WF and IP. In
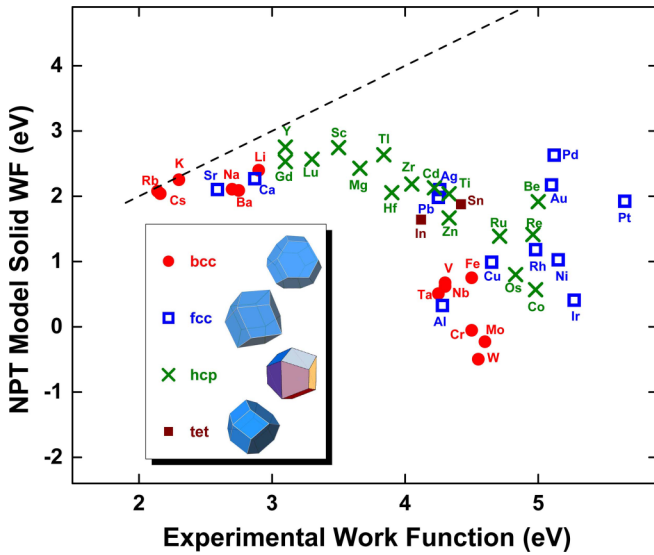
*rtung@brooklyn.cuny.edu
†leeor.kronik@weizmann.ac.il

FIG. 1. Work function of NPT solids as a function of the experimental work function for various elemental metals. Inset: shape of the neutral polyhedron for different crystal structures. Note that for a monoatomic primitive unit cell, the neutral polyhedron reduces to the Wigner-Seitz cell. The vertical difference between each point and the dashed line, which marks a slope of 1, is the surface dipole for that metal.

NPT, planes perpendicular to the axes connecting neighboring atoms are used to partition the bulk charge density into nucleus-centered polyhedra that are neutral individually and can be stacked to construct a "model solid" with a charge distribution that is indistinguishable from that in the interior of the real solid (for examples see inset of Fig. 1). The NPT model solid defines a unique bulk reference, in the sense that the position of its energy bands with respect to the vacuum level is independent of surface orientation and structure. Furthermore, it can be shown (see Supplemental Material, Ref. [29], for proof) that a model solid thus assembled is "fundamental" or "irreducible" in that it has the highest average electrostatic potential energy (i.e., the energy bands of an NPT model solid are positioned at the highest possible point against the vacuum level) among all possible model solids that lead to a surface-independent result. Electrostatically, this is because the electric fields generated by the charge distribution of a neutral polyhedron are maximally confined.

All DFT calculations in this work were performed using a plane-wave basis, along with a projector augmented-wave treatment of core electrons, as implemented in the Vienna *Ab initio* Simulation Package (VASP) [30–32]. Crystal structures and lattice parameters available from the literature were used to calculate the bulk properties of 43 elemental metals, of which those with cubic structures were further optimized in their lattice parameters. A comparison of these lattice parameters with those of ZBD semiconductors identified 11 cubic metals, with lattice mismatches of $\leqslant 2\%$, as suitable for epitaxial interface formation in all three interface geometries discussed below. Additionally, the formation of (110) interfaces was studied for cubic metals with larger lattice mismatches (up to ∼5%), selected cubic-ordered alloys, and several metals with a natural hexagonal lattice but presently

calculated in the fcc structure. Results from these "artificial" interfaces were used mainly to ascertain the validity of conclusions reached from the lattice-matched, realistic systems. Lattice optimization and structure relaxation were conducted with the generalized-gradient approximation functional of Perdew, Burke, and Ernzerhof [33]. Bulk structures and (110) supercells were further computed with the screened hybrid functional of Heyd, Scuseria, and Ernzerhof [34,35]. See Supplemental Material [29] for further details.

The WFs computed for NPT model solids of elemental metals are plotted in Fig. 1 against the experimental work function [36]. The first surprise of this work is the general lack of correlation between the WFs of a metal, with (experimental) and without (NPT) its surface dipole. The NPT-WF does not vary linearly, or even monotonically, with the experimental WF. If anything, there is a reverse trend, in that the NPT-WFs of alkali and alkaline earth metals are generally larger than those of transition metals with large electronegativities. For the latter, metals with similar experimental WFs could vary in their NPT-WFs by more than 3 eV! The difference between the experimental and NPT-based WFs of a metal is, by definition, the surface dipole, D_M (see Fig. 1), which arises from the quantum-mechanical decay of the electron density beyond the surface. We found the surface dipole not to vary simply with the WF, but to vary approximately linearly with the "intermediate" density [26,28], ρ_M^{itm}, of the solid, which is the volumetric electron density at the surface of the NPT model solid (see Supplemental Material [29] for details).

Because the experimental SBH usually varies linearly with the metal WF, one may doubt the relevance of the NPT for SBH theory. However, NPT's immense advantages are revealed once it is actually used to analyze SBHs. A large number of relaxed (110) and (100) interfaces between various semiconductors in the ZBD structure and a selection of the above metals and binary alloys were calculated (see Supplemental Material [29] for details). Following standard DFT procedure [37], SBHs were extracted from supercell calculations as the difference between the Fermi level and the position of the bulk valence-band maximum, when mapped onto the average electrostatic potential in the semiconductor portion of the supercell. Independently, semiconductor IP and metal WF for the corresponding free surfaces were extracted from free-slab calculations. SBH results depend strongly on the type of interface and we begin with the easier, nonpolar (110) interface. Figure 2(a) shows a conventional plot, where the computed SBHs are presented against the SMT prediction. Little correlation is found. Specifically, SBHs for electropositive metals, which have not been studied much previously, fall very significantly below the SMT prediction. Figure 2(b) shows the same computed SBH data replotted against the difference between IP and WF of the semiconductor and metal NPT model solids, respectively. The second surprise of this work is that a clear systematic trend is immediately apparent when surface dipoles are removed.

Inspired by these dramatic improvements, we rewrite Eq. (1) in terms of NPT-based IP and WF,

$$\Phi_{B,p} = I_{SC}^{NPT} - \phi_M^{NPT} + \Delta_{IID}, \qquad (2)$$

where Δ_{IID}, the irreducible interface dipole (IID), is a correction due to charge rearrangement at the interface. It is
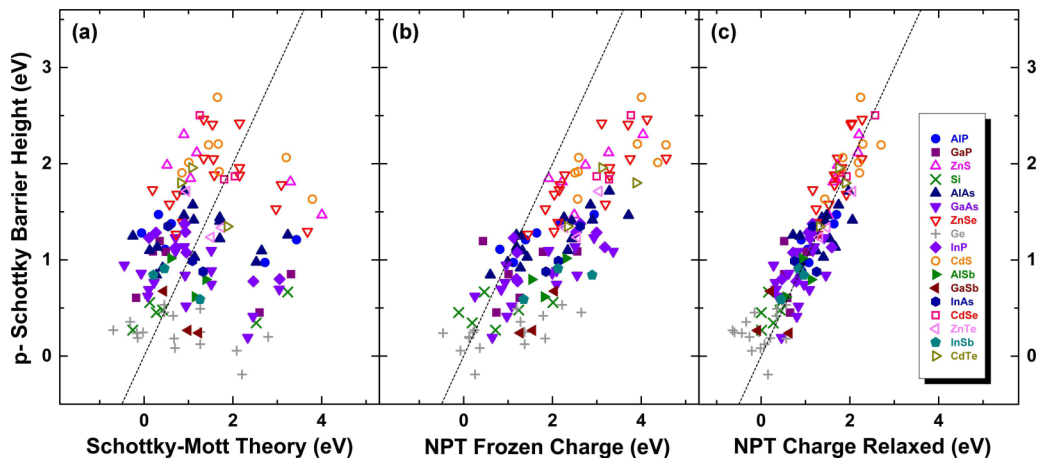
FIG. 2. *p*-type SBHs, calculated using supercells for relaxed epitaxial metal/ZBD (110) interfaces, as a function of the prediction of: (a) Schottky-Mott theory, (b) NPT without interface dipole, (c) NPT with an irreducible interface dipole. Lines denote perfect agreement.

called "irreducible" because the bulk references are so. This marks a different beginning point for SBH analysis. Now that the analysis is free from surface-dipole contributions, the IID is a property entirely of the interface and thus may be amenable to simple chemical modeling. For semiconducting or insulating heterojunctions, the IID was previously found to be relatively modest and could be reasonably approximated as arising from the difference in the average surface charge densities of the two model solids, smoothed out over a distance characteristic of the bond length [26,28]. It is difficult to estimate IID for MS interfaces the same way, because, unlike before, the neutral polyhedra for metals and semiconductors are dissimilar in shape and do not join seamlessly. We therefore assume the following contributions to IID (see Supplemental Material [29] for details): (1) the bond polarization dipole inspired by Pauling, which is proportional to the product of the average electronegativity difference across the interface, the interface distance, and the areal density of bonds. The same fitting parameter is used for all interfacial bond polarization corrections. (2) The charge-transfer dipole, arising from charge-density differences across the interface, which is proportional to $\rho_M^{\mathrm{itm}} - \rho_{SC}^{\mathrm{itm}}$, scaled by the overall ratio of dipole to density, $(D_M + D_{SC})/(\rho_M^{\mathrm{itm}} + \rho_{SC}^{\mathrm{itm}})$, where "SC" denotes "semiconductor." The assumed linear dependence of this dipole on the density difference is strongly suggested by the linearity displayed in Fig. SM-1 of Supplemental Material [29]. In a nutshell, this assumes that the formation of SBH is controlled by bond formation, i.e., chemistry, over a single interplanar distance.

Fitting the two terms to the DFT data for lattice-matched supercells results in the plot of Fig. 2(c), with an rms error of 0.27 eV. Importantly, this is a *global* fit, and not a series of individual fits for each semiconductor. As a result, the obtained coefficients can be used to estimate the SBH for any additional systems. As a demonstration, the coefficients obtained from fitting with lattice-matched systems are shown in Fig. 2(c) to well reproduce/predict the SBHs for artificial interfaces, with large lattice mismatches, included in the same plot. This constitutes the third pleasant surprise of this work: SBHs of various metals on 17 different semiconductors can be quantitatively explained on one universal plot from the

same set of density-based physical and chemical arguments. Previously, SBH analysis could only be conducted for each semiconductor individually, with two fitting parameters each (the CNL and the interface-behavior parameter) that vary with the semiconductor [38]. One further notices that none of the inputs to the present IID estimation (except perhaps the global proportionality constants) requires interface calculation. Therefore, any SBH magnitude, irrespective of the identity of the metal or the semiconductor, can be quantitatively understood from a consideration of basic chemistry, once the surface-dipole stumbling block is removed. Clearly, there is no need for empirical assumptions [4,8].

Turning to the relaxed (100) interfaces, we first note that the SBH depends significantly on whether metal-cation or metal-anion bonds are present at the interface, in agreement with previous investigations [18,19]. Calculations also agree with the measured SBHs for the few interfaces that have been experimentally studied [39,40]. Generally, for a large-WF metal the *p*-type SBH for the metal-anion interface exceeds that of the metal-cation interface, but the reverse is true for small-WF metals. Since the physical and chemical mechanism for SBH formation cannot be different for different interfaces, the method described above for the (110) interfaces should be able to explain the entire spectrum of the more complex (100) SBHs. This, however, requires some further consideration. We begin with the more straightforward metal-anion interfaces. As shown in Fig. 3(a) (open symbols), supercell-calculated SBH compares poorly with that predicted by conventional SMT, and there is, in fact, a weak reverse correlation. As before, the use of NPT-based quantities [Fig. 3(b)] results in a correct systematic trend. The same approach as above (see Supplemental Material [29] for details) is then used to estimate the IID, leading to the open symbols in Fig. 3(c), in good quantitative agreement with theory.

The successful modeling of the IID with bond polarization/charge transfer for the (110) and the metal-anion (100) interfaces, as well as previously for heterojunction interfaces [26], requires that the charge transfer at the interface is extremely short ranged. Previous studies of MS interfaces have estimated the length of interface dipole qualitatively, through layer-by-layer comparison of the potential or density of states
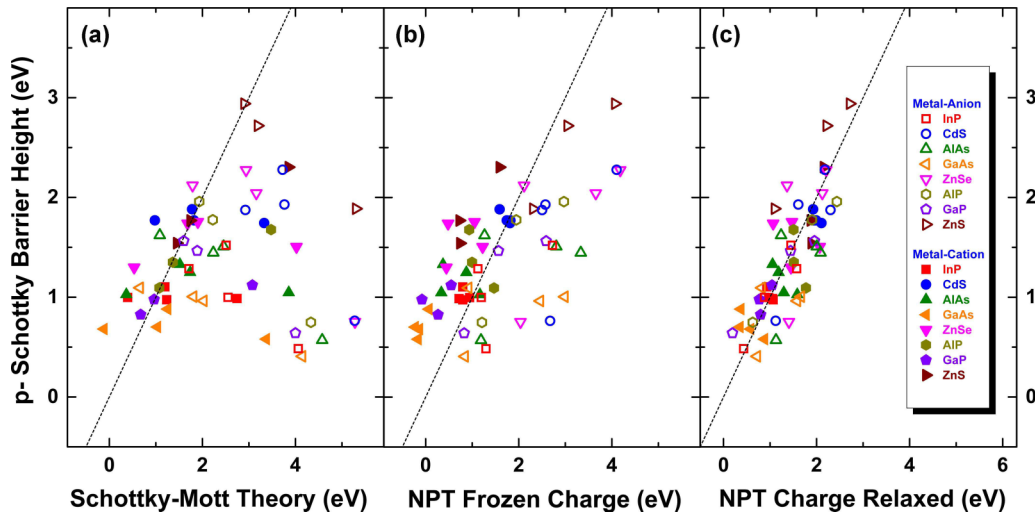
FIG. 3. *p*-type SBHs, calculated using supercells for relaxed epitaxial metal-anion (open symbols) and metal-cation (filled symbols) /zinc-blende (100) interfaces, as a function of the prediction of: (a) Schottky-Mott theory, (b) NPT without interface dipole, (c) NPT with an irreducible interface dipole. Lines denote perfect agreement.

near the interface to bulk references [3,13,21,22]. It can be shown that physically cutting the supercell into segments and "stitching together" the potentials from the separate segment calculations offers a quantitative way for determining the range of charge transfer [41]. Application of this analysis to metal-anion (100) interfaces shows that the interface dipole is indeed extremely short ranged, explaining the success and justifying the use of bond polarization to model these SBHs. The same analysis, however, reveals that the majority of metal-cation (100) interfaces exhibit charge transfer on a longer scale, extending beyond the interface cation plane and into the next anion plane.

The reason for the markedly different behavior of the (100) metal-cation interface is the metallic nature of the metal-cation bond, according to various analyses [41]. Because cations of zinc-blende semiconductors are metallic themselves, the metal-cation bond significantly damps out the effect of the underlying metal, leaving the SBH relatively insensitive to the metal WF. Therefore, the effective "metal" for the metal-cation interface does not end until the first layer of cations is included, such that the semiconductor begins with the next anion plane. With the effective location of the electronic MS interface shifted, the modeling/prediction of the SBH should be conducted between the cation and the anion planes. NPT still properly represents the bulk semiconductor here, but it is no longer the appropriate bulk reference for the metal, which is now "metal covered with cation monolayer." We proceed, in the spirit of the NPT, by computing a reference solid consisting of the metal crystal embedded with two monolayers of cations, as illustrated in Fig. 4. Separating this structure along proximity-cell boundaries [3] between the two monolayers leads to two neutral surfaces of cation-covered metal, terminating on polyhedron facets (see Supplemental Material [29] for discussion). The WF of such a model solid is used as ϕ_M^{NPT} in the analysis of metal-cation interfaces via Eq. (2). SBH of the metal-cation (100) interfaces can be seen from Fig. 3(a) (filled symbols) to compare poorly with SMT prediction. The removal of surface dipole from the IP

and WF significantly improves the agreement, as shown in Fig. 3(b). The IID, which is now between the cation and the anion planes, is then trivially modeled as proportional to the difference in surface dipoles, $D_M - D_{sc}$. Upon linear fitting, the fourth surprise of this work is that good quantitative agreement can be obtained for the entire complicated spectrum of polar (100) SBHs [Fig. 3(c) has an rms error of 0.37 eV]. Finally we note that, being the product of the same NPT and IID procedures, data for corresponding panels of Figs. 2
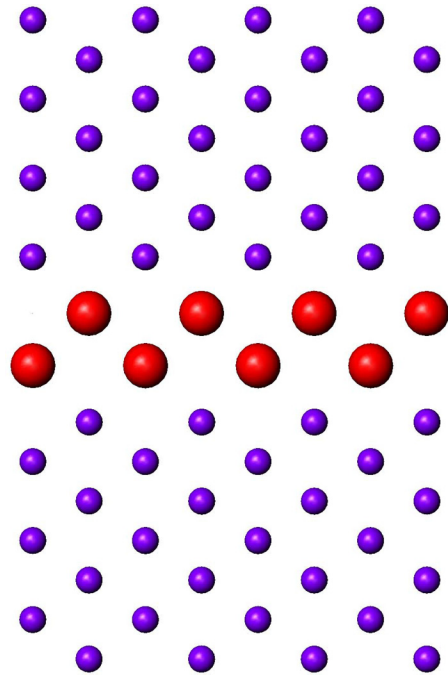

FIG. 4. Schematic representation of the structure used to generate an approximate bulk reference for metal covered with a monolayer of cations. Two cation layers (large symbols) are embedded in a crystal of metal (small symbols).

and 3 can be merged into a single orientation-independent plot, which we avoided doing only for the sake of clarity in presentation. After all, the underlying mechanism of SBH formation should be, and is indeed found to be, independent of interface orientation.

To summarize, an electron-density based theory of the Schottky barrier, in accordance with general chemistry, has remained elusive prior to this work. A major obstacle to such a theory has been the surface contributions inherently included in the way the SBH is traditionally analyzed, following Schottky-Mott theory. This obstacle is removed in this work, using the recently developed NPT, thereby clearing the way for chemistry-guided modeling. For a large number of epitaxial (110) and metal-anion (100) interfaces, where charge transfer is extremely short ranged, we found that a single approach of NPT combined with a simple estimate of charge polarization and transfer across the interface bonds leads to quantitative explanation of the SBH. For metal-cation (100) interfaces, we found that the metallic nature of the metal-cation bonds damps the influence of the metal WF. By shifting the metal-semiconductor interface to the location between the interface cation plane and the next anion plane, SBHs at such interfaces are also modeled successfully. Taken together, the results obtained in this work clearly illustrate that, in order to understand the SBH quantitatively, only the use of appropriate bulk references and simple chemical concepts is required.

[1] S. M. Sze and K. K. Ng, *Physics of Semiconductor Devices,* 3rd ed. (John Wiley and Sons, Hoboken, NJ, 2007).

[2] L. J. Brillson, *Surfaces and Interfaces of Electronic Materials* (Wiley-VCH, Weinheim, 2010).

[3] R. T. Tung, Appl. Phys. Rev. **1**, 011304 (2014).

[4] W. E. Spicer, I. Lindau, P. Skeath *et al.*, J. Vac. Sci. Technol. **17**, 1019 (1980).

[5] A. B. McLean and R. H. Williams, J. Phys. C **21**, 783 (1988).

[6] J. R. Waldrop, Appl. Phys. Lett. **44**, 1002 (1984).

[7] J. Bardeen, Phys. Rev. **71**, 717 (1947).

[8] J. Tersoff, Phys. Rev. Lett. **52**, 465 (1984).

[9] M. Cardona and N. E. Christensen, Phys. Rev. B **35**, 6182 (1987).

[10] R. T. Tung, Phys. Rev. Lett. **52**, 461 (1984).

[11] R. T. Tung, A. F. J. Levi, J. P. Sullivan, and F. Schrey, Phys. Rev. Lett. **66**, 72 (1991).

[12] C. J. Palmstrom, T. L. Cheeks, H. L. Gilchrist *et al.*, J. Vac. Sci. Technol. A **10**, 1946 (1992).

[13] H. Fujitani and S. Asano, Phys. Rev. B **42**, 1696 (1990).

[14] H. Palm, M. Arbes, and M. Schulz, Phys. Rev. Lett. **71**, 2224 (1993).

[15] A. Olbrich, J. Vancea, F. Kreupl *et al.*, Appl. Phys. Lett. **70**, 2559 (1997).

[16] R. T. Tung, Phys. Rev. B **45**, 13509 (1992).

[17] J. P. Sullivan, R. T. Tung, M. R. Pinto *et al.*, J. Appl. Phys. **70**, 7403 (1991).

[18] R. G. Dandrea and C. B. Duke, J. Vac. Sci. Technol. B **11**, 1553 (1993).

[19] C. Berthod, N. Binggeli, and A. Baldereschi, Phys. Rev. B **68**, 085323 (2003).

[20] S. Picozzi, A. Continenza, G. Satta, S. Massidda, and A. J. Freeman, Phys. Rev. B **61**, 16736 (2000).

[21] M. Nunez and M. Buongiorno Nardelli, Phys. Rev. B **73**, 235422 (2006).

[22] M. Mrovec, J. M. Albina, B. Meyer, and C. Elsasser, Phys. Rev. B **79**, 245121 (2009).

[23] Y. Takei and T. Nakayama, Jpn. J. Appl. Phys. **48**, 081001 (2009).

[24] W. Schottky, Z. Phys. **113**, 367 (1939).

[25] N. F. Mott, Proc. R. Soc. London **A171**, 27 (1939).

[26] R. T. Tung and L. Kronik, Phys. Rev. B **94**, 075310 (2016).

[27] R. T. Tung and L. Kronik, Adv. Theo. Simul. **1**, 1700001 (2018).

[28] R. T. Tung and L. Kronik, Phys. Rev. B **99**, 115302 (2019).

[29] See Supplemental Material at http://link.aps.org/supplemental/10.1103/PhysRevB.103.035304 for Summary of pertinent aspects of neutral polyhedra theory; Correlation between surface dipole and surface volumetric charge density for metals; Additional information on SBHs of non-polar (110) metal-semiconductor interfaces; Details of DFT supercell calculations; Chemical modeling of the irreducible interface dipole; Additional information on SBHs of (100) metal-semiconductor interfaces; Tabulated metal, semiconductor, and metal/semiconductor data.

[30] G. Kresse and J. Hafner, Phys. Rev. B **49**, 14251 (1994).

[31] G. Kresse and J. Furthmuller, Phys. Rev. B **54**, 11169 (1996).

[32] G. Kresse and D. Joubert, Phys. Rev. B **59**, 1758 (1999).

[33] J. P. Perdew, K. Burke, and M. Ernzerhof, Phys. Rev. Lett. **77**, 3865 (1996).

[34] J. Heyd, G. E. Scuseria, and M. Ernzerhof, J. Chem. Phys. **118**, 8207 (2003).

[35] A. V. Krukau, O. A. Vydrov, A. F. Izmaylov *et al.*, J. Chem. Phys. **125**, 224106 (2006).

[36] H. B. Michaelson, J. Appl. Phys. **48**, 4729 (1977).

[37] M. Peressi, N. Binggeli, and A. Baldereschi, J. Phys. D **31**, 1273 (1998).

[38] R. T. Tung, Mater. Sci. Eng. Rep. **35**, 1 (2001).

[39] A. Y. Cho and P. D. Dernier, J. Appl. Phys. **49**, 3328 (1978).

[40] W. I. Wang, J. Vac. Sci. Technol. B **1**, 574 (1983).

[41] R. T. Tung and L. Kronik (unpublished) (2020).